Combining the Fluctuating Charge Method, Non-periodic Boundary Conditions and Meta-dynamics: Aqua Ions as Case Studies

ARTICLE *in* JOURNAL OF CHEMICAL THEORY AND COMPUTATION · FEBRUARY 2014

Impact Factor: 5.5 · DOI: 10.1021/ct400988e

3 AUTHORS, INCLUDING:

Giordano Mancini
Scuola Normale Superiore di Pisa
56 PUBLICATIONS **530** CITATIONS
SEE PROFILE

Vincenzo Barone
Scuola Normale Superiore di Pisa
775 PUBLICATIONS **44,810** CITATIONS
SEE PROFILE

THE JOURNAL OF PHYSICAL CHEMISTRY Letters

Letter

pubs.acs.org/JPCL

In Silico Study of Molecular-Engineered Nanodevices: A Lockable Light-Driven Motor in Dichloromethane Solution

Costantino Zazza,* Giordano Mancini, Giuseppe Brancato, and Vincenzo Barone

Scuola Normale Superiore di Pisa, P.zza dei Cavalieri 7, 56126 Pisa, Italy

Supporting Information

ABSTRACT: A light-driven molecular rotor, featuring an acid−base-triggered self-complexing lock in dichloromethane dilute solution, is investigated for the first time by an integrated computational strategy allowing a quantitative reproduction of all of the main experimental features in terms of a comprehensive and interpretable molecular picture. In particular, we have simulated the peculiar conformational preferences of the rotor in two different protonation states, characterized the free-energy landscape that drives the threading→dethreading motion, and then reproduced the available spectroscopic data under equilibrium conditions. Interestingly, we also observed that the confinement of the $R_2NH_2^+$ arm within the [1]pseudorotaxane moiety actually inhibits the cis−trans isomerization within the photoactive xanthene//2,6-dioxonaphthalene unit, creating a friction (resistance) against the threading→dethreading motion. Together with the specific interest of the studied system, this contribution highlights the potentialities of modern computational techniques to fully simulate complex and flexible devices in which noncovalent forces can finely modulate energy-conversion schemes working at the nanoscale level.

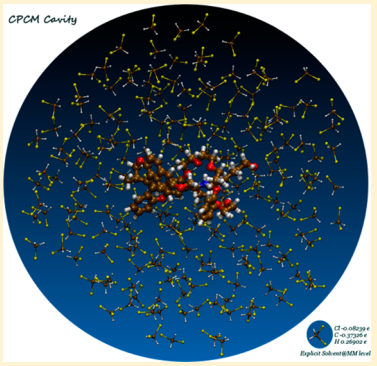

SECTION: Physical Processes in Nanomaterials and Nanostructures

Nanotechnology is aimed at the use of small molecular assemblies, or even individual molecules, as functional building blocks in the construction of advanced devices and machines.[1−6] Single-molecule devices appear to be ideal candidates in this field because they allow high densities and because their flexible structure may pave the route toward novel intrinsic functionalities. The trend is to classify the molecular devices in two domains: Brownian and stimuli-responsive.[7−9] The first domain collects systems in which the switching mechanisms are governed by thermal fluctuations in non-equilibrium state;[10,11] on the other hand, the term stimuli-responsive is used in the case of conformational changes driven by external forces.[1−6,12−14] In particular, systems showing quasi 1-D fluctuations under ad-hoc perturbations (e.g., chemical reactions, pH-variation, electrochemical reduction, UV−vis radiation) result in being attractive as prototypical units for stimuli-responsive devices.[1−9] In this context, the driving forces controlling the shaping and function of biological machinery, such as molecular recognition, self-assembly, and multivalency, have been employed in template-directed synthesis with the idea to realize artificial motors capable of converting chemical energy into structural transitions.[1−6,15,16] Importantly, the literature in this field also aims at understanding the chemical properties of complex systems in confined subspaces, as well as the impact that internal motions with various degrees of complexity might have in today's and next generation's materials.

While contemporary experimental techniques are able to provide a wealth of detailed results, their interpretation in molecular terms requires reliable yet effective multiscale modeling.[17−22] Here, in the context of artificial devices, we report on a computational study of a recently proposed light-driven molecular rotor, featuring an acid−base-triggered self-complexing lock in dichloromethane.[23] Such a rotor was selected as a realistic model to demonstrate the ability of modern computational techniques to fully simulate the chemical and spectroscopic behavior of complex nanoscale devices in their operating environment and to further unravel new insights into their working principle. The original experimental work by Qu and Feringa[23] showed that the presence of a [1]pseudorotaxane unit, composed of a dibenzo[24]crown-8 (DB24C8) ring in interaction with a secondary dialkylammonium ($R_2NH_2^+$) moiety can inhibit a cis−trans isomerization along the C═C double bond, as magnified in Scheme 1. The same authors[23] have then realized a single-molecule system in which a rotating arm, when protonated, acts as a plug for a socket formed by a DB24C8 ether; the designed molecular rotor results locked via electrostatic interactions without showing any rotational movement, even if exposed to light and thermal cycles. Once the $R_2NH_2^+$ unit is deprotonated, the system is unlocked and the socket can be unplugged upon irradiation.[23] Here we report the main results of a comprehensive computational study of the thermodynamic and kinetic properties of the locking−unlocking mechanism driving the functionality of the nano-device. Moreover, available spectroscopic data have been

Received: September 10, 2013
Accepted: November 1, 2013

   dx.doi.org/10.1021/jz4019404 | J. Phys. Chem. Lett. 2013, 4, 3885−3890

Scheme 1. Chemical Structures of the Self-Complexing, Acid–Base-Controllable Molecular Rotor, as Reported in Ref 23

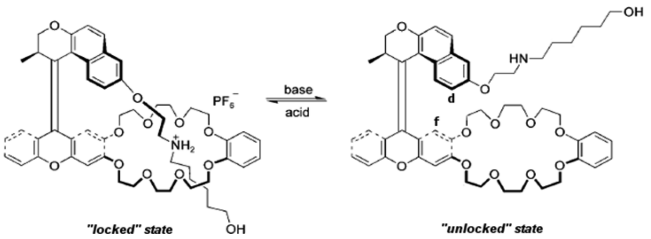

reproduced to further and better validate our computational model. In our investigation, we have only marginally analyzed the photoinduced cis–trans isomerization occurring in the excited state, which is of minor interest in the present context and can be regarded as a distinct process. To be specific, we exploited a series of computational approaches by combining both equilibrium and nonequilibrium classical molecular dynamics (MD) simulations with quantum mechanical methods based on density functional theory (DFT).[22] Inspired by the experimental protocol and with the intention to shed further light on the working mechanism of the present rotor, we focus here on: (1) the identification of the conformational space accessible under thermal energy and modulated via noncovalent interactions; (2) the quantitative estimation of the free-energy profiles driving the locking–unlocking (L-U) mechanism; and (3) the characterization of the molecular orbitals promoting the cis–trans isomerization upon irradiation.

In line with experimental findings,[23] we have carried out two 100 ns MD simulations with the functionalized molecular arm in the threaded (in the case of the protonated form) and dethreaded (neutral form) configurations, respectively. First, to address the stability of the intramolecular self-complexation in the [1]pseudorotaxane subsystem, we have monitored the distance between the center of mass (COM) of the DB24C8 ring and the nitrogen atom in the molecular thread (hereafter referred to as $R_{\text{N-DB24C8}}$) along MD simulations of both covalent frameworks, namely, the charged and neutral states, performed at room temperature. The comparison of both forms shows that the neutral one is highly flexible, with $R_{\text{N-DB24C8}}$ distances ranging from 6 to 17 Å, as plotted in Figure 1. In such a case, the nanodevice only samples unlocked conformations, in which the R_2NH arm is mainly surrounded by the solvent and is free to fluctuate according to thermal energy. On the contrary, the protonated form remains locked within the DB24C8 moiety during the entire simulation time. Therefore, in a solvent that does not disrupt H-bonding contacts, the $R_2NH_2^+$ ion and the crown ether do exhibit a favorable electrostatic network, which has the effect of hindering any significant structural flexibility. The distributions depicted in Figure 1 (lower left panel) show that the protonated form is characterized by a very narrow distribution of the $R_{\text{N-DB24C8}}$ distance with a maximum lying at almost 1 Å, whereas the neutral rotor presents a rather broad distribution peaked at 14

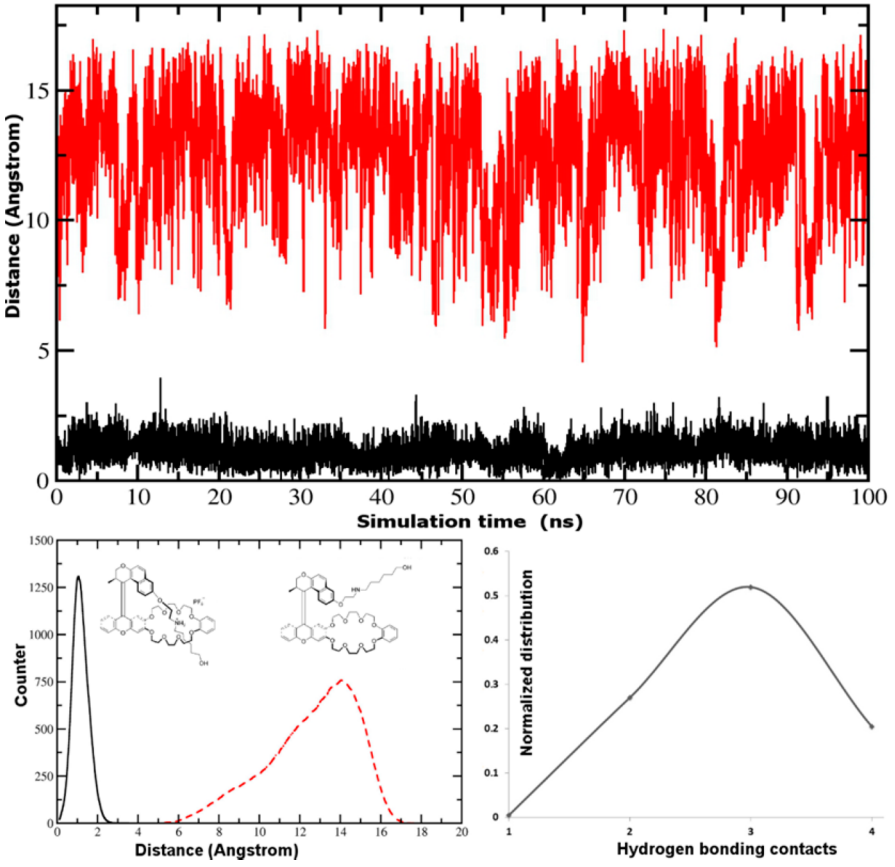

Figure 1. Upper panel: R_N-DB24C8 distance as extracted from the 100 ns MD at 298 K in CH_2Cl_2; DB24C8– $R_2NH_2^+$ (black line), DB24C8-R_2NH (red line). Lower-left: distributions of the DB24C8– $R_2NH_2^+$ (black line) and DB24C8-R_2NH (red dashed line) distances; lower-right: normalized distribution of the H-bond contacts between the $R_2NH_2^+$ and the DB24C8.

dx.doi.org/10.1021/jz4019404 | J. Phys. Chem. Lett. 2013, 4, 3885–3890

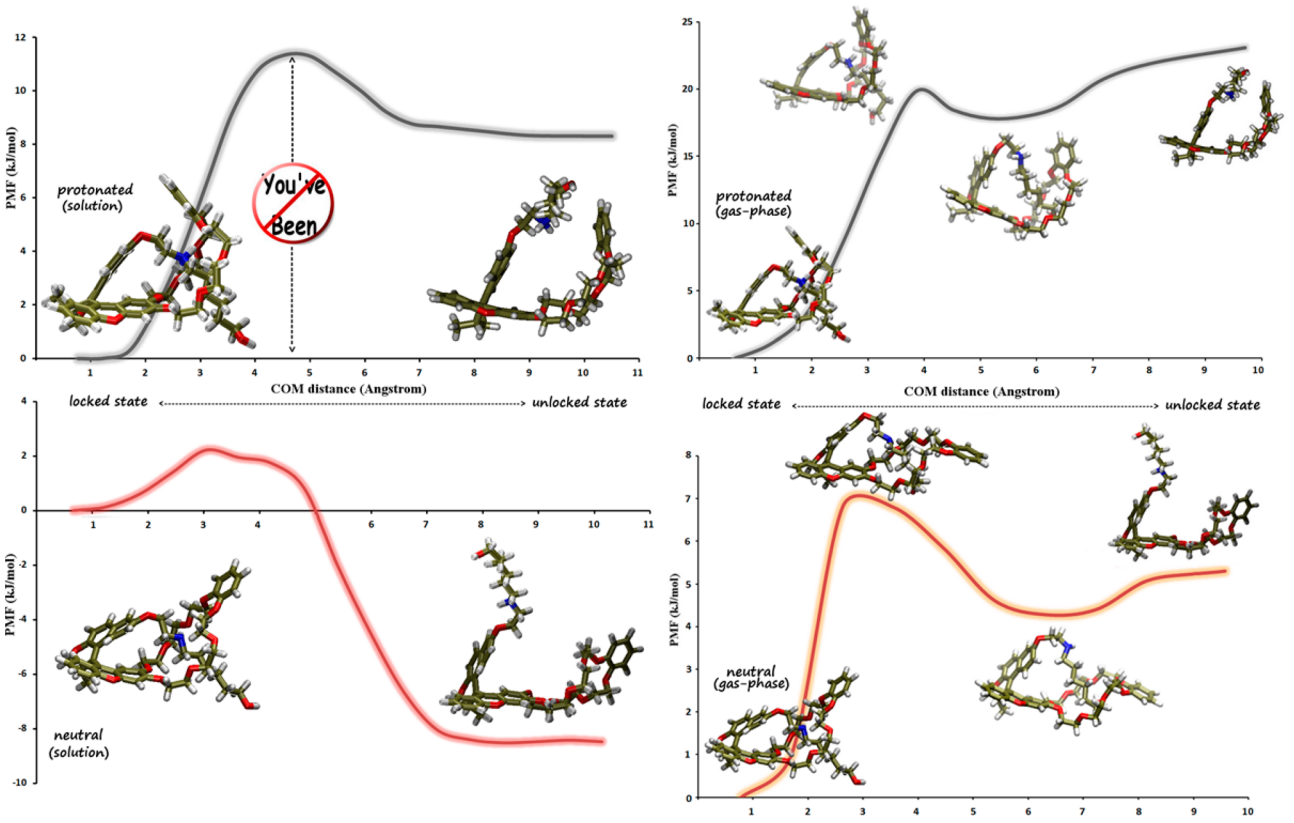

Figure 2. Left panel: Free-energy profiles of the molecular rotor along the L→U coordinate (see the text) in CH_2Cl_2 dilute solution; the upper panel refers to the protonated form ($R_2NH_2^+$), while the lower panel refers to the neutral one (R_2NH). Right panel: the same as left panel but for the L→U coordinate in the gas phase.

Å with a full-width at half-maximum larger than 5 Å. Still analyzing the MD results, the self-complexation can be attributed to the formation of up to four H bonds ($N^+H\cdots OR_2$) that tend to stabilize the [1]pseudorotaxane moiety into a "locked" subspace (lower-right panel). To be more specific, by using a simple cutoff distance of 3.0 Å for the definition of hydrogen bonding, we found that the $R_2NH_2^+$ molecular thread always forms at least two hydrogen bonds with the DB24C8 ether ring, which during most of the overall simulation (75% of the total time) actually become three or four (see Figure 1, lower right panel and Figures S2a,b in the Supporting Information). In particular, the three H-bond configuration does correspond to three strong hydrogen bonds (<3.0 Å) plus an additional "weak" H bond showing distances in the range of 3.0 to 3.3 Å. It is worth noting that, while the specific H-bond distribution so obtained is affected by the arbitrariness of the distance criterium, our analysis does show unequivocally a locking site constrained but still capable of small structural rearrangements. Note that the atomic point charges of the rotor were refined at DFT level and kept fixed during the MD simulations (Figure S5, see also subsection 1.1 in the Supporting Information for further details).

Moreover, in an attempt to characterize energetically the L-U mechanism of the rotor, the free-energy profile along the "dethreading" motion, that is, the coordinate describing the self-complexing lock in the [1]pseudorotaxane (see Scheme 1), was evaluated by a series of umbrella sampling simulations both in dichloromethane and in vacuo.[24−26] In CH_2Cl_2 solution, as far as the protonated form is concerned, the estimated trend reported in Figure 2 (left panel) shows a significant penalty accompanying the interconversion of the locked→unlocked state of ∼11.3 kJ/mol at a distance of 4.5 Å. At the same time, the computed free-energy profile also evidences the spontaneous character of the intramolecular self-complexing lock in CH_2Cl_2 solution at 298 K: at distances larger than 7 Å, a flat (positive) profile is obtained, with a free-energy increase of ∼8.3 kJ/mol with respect to the locked configuration. The deprotonated form shows an L→U energy barrier lower than thermal energy (∼2.2 kJ/mol at 3.0 Å) and, most importantly, an unlocked state more favorable than its locked counterpart by 8.5 kJ/mol. Overall, the present free-energy analysis nicely supports the experimental observation about the occurrence of rotatory motions only upon deprotonation of the system and subsequent relaxation toward unlocked structures; remarkably, a relatively small free-energy barrier of the same order of kT is reversibly switched by pH variation so as to stabilize only one of the two conformations in each case: curiously, the two computed free-energy profiles do appear as mirror images of one of the other. Note that the overall energy barrier results from a subtle balance between favorable energetic and entropic contributions concerning both the rotor and the solvent, which should be properly considered for a realistic modeling. In particular, the formation/breaking of the intramolecular H-bonding network, as previously described, and the solvent stabilization of the protonated form do play a crucial role in triggering the observed L-U mechanism. Indeed, such a picture is drastically changed in the gas-phase, where the locked structure is invariably the most stable one irrespective of the protonation state of the arm, even if to a different extent (see Figure 2, right panel). For the sake of completeness, it is also worth noting that, as observed experimentally, in a more polar solvent, that is, dimethyl sulfoxide, the present synthetic device

dx.doi.org/10.1021/jz4019404 | J. Phys. Chem. Lett. 2013, 4, 3885−3890

has shown no indication of a stable intramolecular [$R_2NH_2^+$ DB24C8 ether] self-complexation pattern.[23] Therefore, it may be concluded that the role of the solvent is absolutely essential to determine an efficient L-U mechanism: both high and extremely low polar solvents overstabilize either the unlocked or the locked configuration, respectively, thus inactivating the L-U mechanism; apparently, only moderately polar solvents are able to provide a differential free-energy landscape between the neutral and the protonated forms of the amino moiety.

To proceed further, the spontaneous dethreading of the rotor arm upon $R_2NH_2^+$ deprotonation in CH_2Cl_2 has been successfully reproduced by nonequilibrium MD simulations without introducing any restraint in the system. In the present context, we have implicitly assumed that the investigated device in the neutral form initially samples threaded conformations; please note that this imposed condition resembles the experimental scenario following the addition of 1,8-diazabicyclo-[5.4.0]undec-7-ene (DBU)[23] to deprotonate the dialkylammonium ion moiety. A set of five 20 ns MD simulations at 298K, starting from uncorrelated structures of the locked and neutral species, have been carried out, invariably showing the aptitude of this system to transduce a selective acid−base variation into a fully coupled dethreading motion occurring on the nanosecond time-scale: within the simulated time interval (20 ns), in a range between 3 to 16 ns, all trajectories have reproduced the complete unlocking of the rotor arm. (See Figure 3 and the Supporting Information for further details.)

Again, the physical behavior of such a molecular lock, as emerged from the previous computational findings, nicely

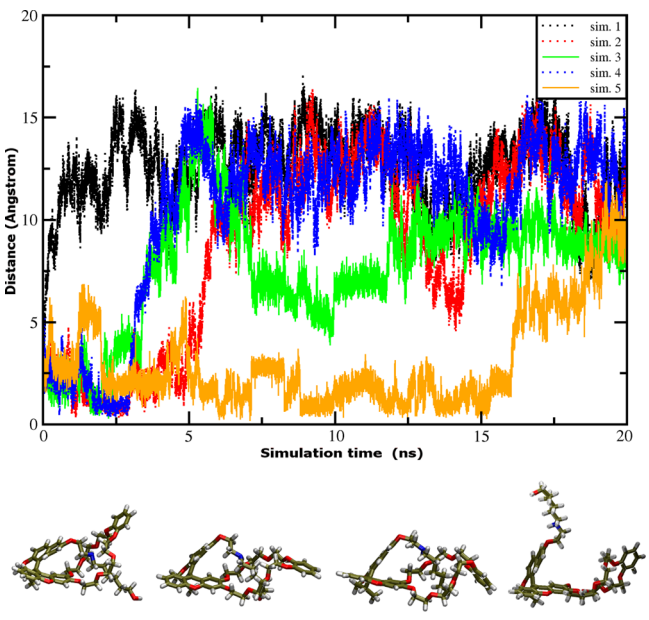

Figure 3. Upper panel: $R_{N\text{-}DB24C8}$ distance along the simulation time (20 ns MD sampling at 298 K in CH_2Cl_2); it should be noted that to verify that the investigated device can efficiently unlock the [1]pseudorotaxane moiety when deprotonated, we considered five different MD simulations under nonequilibrium conditions starting from locked conformations. (See the text.) The unlocking probability averaged over the classical trajectories is found to be equal to 1 when the simulation time reaches 16 ns. Lower panel: some snapshots showing the spontaneous conformational rearrangement bringing to the unlocking (from left to right) of the investigated synthetic rotor. Note that for the sake of clearness the solvent molecules have been omitted.

matches the picture proposed in ref 23 based on the comparison of ^{1}H NMR and UV/vis spectra acquired under the same conditions. Hence, we decided to fully characterize such a system, from the computational viewpoint, by reproducing the spectroscopic data considered in the experimental interpretation. By comparing the minimum energy conformations of the protonated/deprotonated forms, the DFT-predicted ^{1}H NMR chemical shift changes for H_d (−0.3 ppm) and H_f protons (−0.6 ppm) were found in remarkable agreement with the measured downfield of −0.3 and −0.5 ppm, respectively. (See Scheme 1.)[23]

Moreover, considering the charged species in CH_2Cl_2 at low temperature, the UV/vis absorption band, lying at ca. 370 nm, has also been computed by averaging the excitation energy over a set of 40 equally spaced configurations (a snapshot every 0.5 ns), as extracted from a 20 ns MD trajectory carried out at 253 K. (See Figure 4.) We performed such a new MD simulation

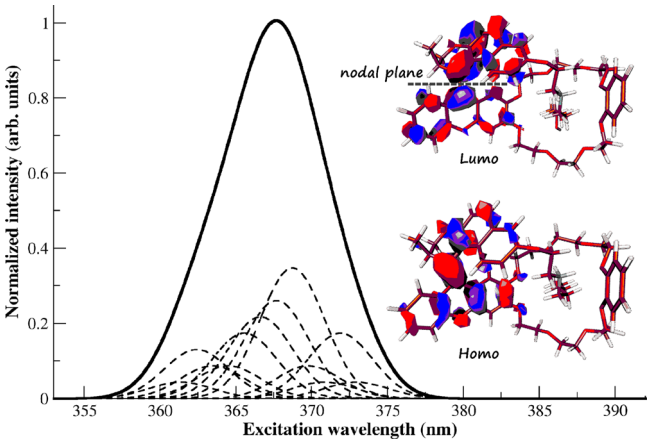

Figure 4. Lowest UV/vis band, at the [Cam-B3LYP/6-31+G-(3df,2pd)//6-31G(d,p)+MM+C-PCM] level, of the protonated rotor in CH_2Cl_2 solution from 40 equally spaced all-atom MD (20 ns@253K) frames. The molecular orbitals involved in the excitation process are also depicted.

with the aim of matching the experimental conditions[23] applied during UV/vis spectroscopical measurements over the protonated species confined within its deep free-energy minimum basin (e.g., threaded form, see Figures 1 and 2). For each snapshot, time-dependent DFT (TD-DFT) calculations were carried out by employing an asymptotically corrected hybrid functional, namely, Cam-B3LYP,[27] and two atomic basis sets [i.e., 6-31+G(3df,2pd)//6-31G(d,p)].[22] To be more specific, the xanthene and 2,6-dioxonaphthalene units were both treated using the 6-31+G(3df,2pd) basis set, whereas the remaining covalent framework was modeled at the 6-31G(d,p) level. All solvent molecules within a cutoff distance of 25 Å from the solute center of mass were treated (explicitly) at the classical level,[28] and the polarizable continuum model (PCM)[29,30] was used to account for the long-range interactions with the environment. It is remarkable that test calculations carried out imposing larger spherical samples (cutoff distanced of 28 and 30 Å) did not shown significant differences in the excitation energy. Note that the choice of TD-DFT was based on previous successful applications on similar systems in nonaqueous solutions.[17−21] The computed absorption band agrees well with experiments; the estimated spectrum shows a single peak profile in the range 360−375 nm with λ_{max}= 368 nm. Besides, a molecular orbital analysis has shown that during

dx.doi.org/10.1021/jz4019404 | J. Phys. Chem. Lett. 2013, 4, 3885−3890

the excitation, the electronic structure of the rotor undergoes a clear $^1\pi\rightarrow\pi^*$ transition, in which the C=C bond between the stator and the rotating unit partially loses its double-bond character. As a consequence, only in the case of the neutral form can the photoactive machine be destabilized, inducing, in the excited state, a cis−trans conversion. The simulation results then allow both a qualitative reproduction of the lowest energy UV/vis band and the identification of the electronic degrees of freedom that funnel the 365 nm light pulse into the structure of the synthetic device. Also, our analysis reveals another important aspect that indirectly supports one of the key conclusion in the original work: the lack of any cis−trans isomerization along the double bond connecting the xanthene and 2,6-dioxonaphthalene units after irradiation at 365 nm.[23] It seems reasonable to assume that the presence of an appreciable unlocking barrier (∼4.5 kT; see Figure 2) may allow substantially "vertical" $^1\pi\rightarrow\pi^*$ excitations at ∼365 nm because it should not be largely affected by the local electronic density variation accompanying the lowest UV/vis transition within the photoactive xanthene//2,6-dioxonaphthalene moiety.

In summary, we have been able to reproduce by an integrated computational strategy all of the main experimental results available for a light-driven rotor in CH_2Cl_2, featuring a self-complexing lock under acid−base control. Furthermore, the computational findings have provided a comprehensive molecular picture about the reversible working principle that characterizes such a nanodevice, namely, its locking−unlocking mechanism, which nicely complements and supports the experimental evidence reported in the study by Qu and Feringa.[23] In particular, we have consistently compared the conformational preferences of the two possible protonation states of the synthetic system at finite temperature and different pH. Significant differences in the dynamics and thermodynamics of the protonated and deprotonated forms have emerged, thus corroborating the originally hypothesized picture about the presence of an efficient self-complexing [1]-pseudorotaxane-locking mechanism driven by both pH variation and solvation effects. Remarkably, from molecular simulations, we have been able to show that the confinement of the $R_2NH_2^+$ arm can inhibit the photoinduced switching between cis and trans isomers actually creating a resistance against the dethreading motion of ∼4.5 kT in dichloromethane. The crucial role of the solvent in triggering the L-U mechanism has been further analyzed by considering the same system in vacuo, where only the locked state resulted stable. Therefore, the present contribution reinforces the idea that tailored noncovalent forces in nanodevices can play a wide range of critical effects, which go rather far beyond the simple structure characterization. In addition, the available spectroscopic (NMR and UV/vis) data under equilibrium conditions were satisfactorily reproduced. From a more general point of view, the present work confirms that atomistic simulations can meet advanced experiments and predict the behavior of intriguing and flexible multicomponent molecular devices, thereby enhancing our strategies to exploit their tremendous potential in nanotech applications.

■ ASSOCIATED CONTENT

Supporting Information

Extended computational details section and supplementary results. This material is available free of charge via the Internet at http://pubs.acs.org.

■ AUTHOR INFORMATION

Corresponding Author

*E-mail: costantino.zazza@sns.it. Tel: +39 050 509167. Fax: +39 050 509768.

Notes

The authors declare no competing financial interest.

■ ACKNOWLEDGMENTS

This work was supported by MIUR (FIRB RBFR10DAK6) and by ERC Advanced Grant 2012 (number 320951).

■ REFERENCES

(1) Balzani, V.; Credi, A.; Venturi, M. *Molecular Machines and Devices: Concepts and Perspectives for the Nanoworld*; Wiley-VCH: Weinheim, Germany; 2008.

(2) Jones, R. A. L. *Soft Machines, Nanotechnology and Life*; Oxford University Press: Oxford, U.K., 2004.

(3) Kay, E. R.; Leigh, D. A.; Zerbetto, F. Synthetic Molecular Motors and Mechanical Machines. *Angew. Chem., Int. Ed.* **2006**, *46*, 72−191.

(4) Stoddart, J. F. The Chemistry of the Mechanical Bond. *Chem. Soc. Rev.* **2009**, *38*, 1802−1820.

(5) Feringa, B. Nanotechnology: In Control of Molecular Motion. *Nature* **2000**, *408*, 151−154.

(6) Bell, T. W.; Cline, J. I. Chemical Evolution II: From the Origins of Life to Modern Society, *ACS Symp. Ser.*, Chapter 12, **2010**, *2015*, 233.

(7) Kottas, G. S.; Clarke, L. I.; Horinek, D.; Michl, J. Artificial Molecular Rotors. *Chem. Rev.* **2005**, *105*, 1281−1376.

(8) Silvi, S.; Credi, A. Molecular Motors and Machines. In *Nanotechnology for Biology and Medicine*; Springer: New York, 2012; pp 71−100.

(9) Schliwa, M.; Woehlke, G. Molecular Motors. *Nature* **2003**, *422*, 759−765.

(10) Astumian, D. R. Design Principles for Brownian Molecular Machines: How to Swim in Molasses and Walk in a Hurricane. *Phys. Chem. Chem. Phys.* **2007**, *9*, 5067−5083.

(11) Astumian, D. R. Thermodynamics and Kinetics of a Brownian Motor. *Science* **1997**, *276*, 917−922.

(12) Balzani, V.; Credi, A.; Venturi, M. Molecular Devices and Machines. *NanoToday* **2007**, *2*, 18−25 and quoted references therein cited.

(13) Saha, S.; Stoddart, J. F. Photo-Driven Molecular Devices. *Chem. Soc. Rev.* **2007**, *36*, 77−92.

(14) Volume on "Molecular Machines, *Top. Curr. Chem.* **2005**, *262*, 1-236.

(15) Fang, L.; Olson, M. A.; Benítez, D.; Tkatchouk, E.; Goddard, W. A., III; Stoddart, J. F. Mechanically Bonded Macromolecules. *Chem. Soc. Rev.* **2010**, *39*, 17−29.

(16) Stoddart, J. F. Molecular Machines. *Acc. Chem. Res.* **2001**, *34*, 410−411.

(17) Mancini, G.; Zazza, C.; Aschi, M.; Sanna, N. Conformational Analysis and UV/Vis Spectroscopic Properties of a Rotaxane-Based Molecular Machine in Acetonitrile Dilute Solution: When Simulations Meet Experiments. *Phys. Chem. Chem. Phys.* **2011**, *13*, 2342−2349.

(18) Zazza, C.; Mancini, G.; Brancato, G.; Sanna, N.; Barone, V. Neutral Molecular Shuttle in Acetonitrile Dilute Solution Investigated by Molecular Dynamics and Density Functional Theory. *Comput. Theor. Chem.* **2012**, *985*, 53−61.

(19) Zazza, C.; Amadei, A.; Sanna, N.; Aschi, M. Can a Synthetic Thread Act as an Electrochemically Switchable Molecular Device? *Chem. Commun.* **2008**, *29*, 3399−3401.

(20) Zazza, C.; Mancini, G.; Sanna, N.; Aschi, M. Thermodynamic Features and Environmental Effects in a Two-States Molecular Device Under Strict Electrochemical Control. *Theor. Chem. Acc.* **2009**, *123*, 383−390.

(21) Zazza, C.; Mancini, G.; Amadei, A.; Sanna, N.; Aschi, M. A Fast Redox-Induced Switching Mechanism in a Conformationally Control-

lable Molecular Thread in Solution. *Phys. Chem. Chem. Phys.* **2010**, *12*, 4552−4554.
(22) For a detailed description of the overall computational setup, we invite the reader to refer to the Supporting Information.
(23) Qu, D.-H.; Feringa, B. Controlling Molecular Rotary Motion with a Self-Complexing Lock. *Angew. Chem., Int. Ed.* **2010**, *49*, 1107−1110 also reported in *Chemistry World* magazine in Locking Molecular Motors, February 2010 issue.
(24) Torrie, G.; Valleau, J. Nonphysical Sampling Distributions in Monte Carlo Free-Energy Estimation: Umbrella sampling. *J. Comput. Phys.* **1977**, *23*, 187−199.
(25) S. Kumar, S.; Rosenberg, J. M.; Djamal Bouzida, D.; Swendsen, R. H.; Kollman, P. A. The Weighted Histogram Analysis Method for Free-Energy Calculations on Biomolecules I. The method. *J. Comput. Chem.* **1992**, *13*, 1011−1021.
(26) We selected, as a coordinate, the distance between the geometrical center of the oxygen atoms forming the DB24C8 ring and the COM of the amino group located on the arm. A harmonic restraint potential of 10 kJ mol $^{-1}$ Å^{-2} was applied to confine such a parameter within a region varying from 1 to 10 Å and composed of 20 evenly spaced intervals. For each interval, a 20 ns MD simulation (T = 298 K; p = 1 bar) was carried out for both protonation states for a total time of 800 ns. The first 2 ns was disregarded in the derivation of the potential of mean force (PMF); forces and mutual displacements were stored every 2 ps.
(27) Yanai, T.; Tew, D. P.; Handy, N. C. A New Hybrid Exchange−Correlation Functional Using the Coulomb-Attenuating Method (CAM-B3LYP). *Chem. Phys. Lett.* **2004**, *393*, 51−57.
(28) The liquid CH_2Cl_2 was modeled according to: Dang, D. X.Intermolecular Interactions of Liquid Dichloromethane and Equilibrium Properties of Liquid−Vapor and Liquid−Liquid Interfaces: a Molecular Dynamics Study. *J. Chem. Phys.* **1999**, *110*, 10113-10122.
(29) Tomasi, J.; Mennucci, B.; Cammi, R. Quantum Mechanical Continuum Solvation Models. *Chem. Rev.* **2005**, *105*, 2999−3094.
(30) Cossi, M.; Rega, N.; Scalmani, G.; Barone, V. Energies, Structures, and Electronic Properties of Molecules in Solution with the C-PCM Solvation Model. *J. Comput. Chem.* **2003**, *24*, 669−681.